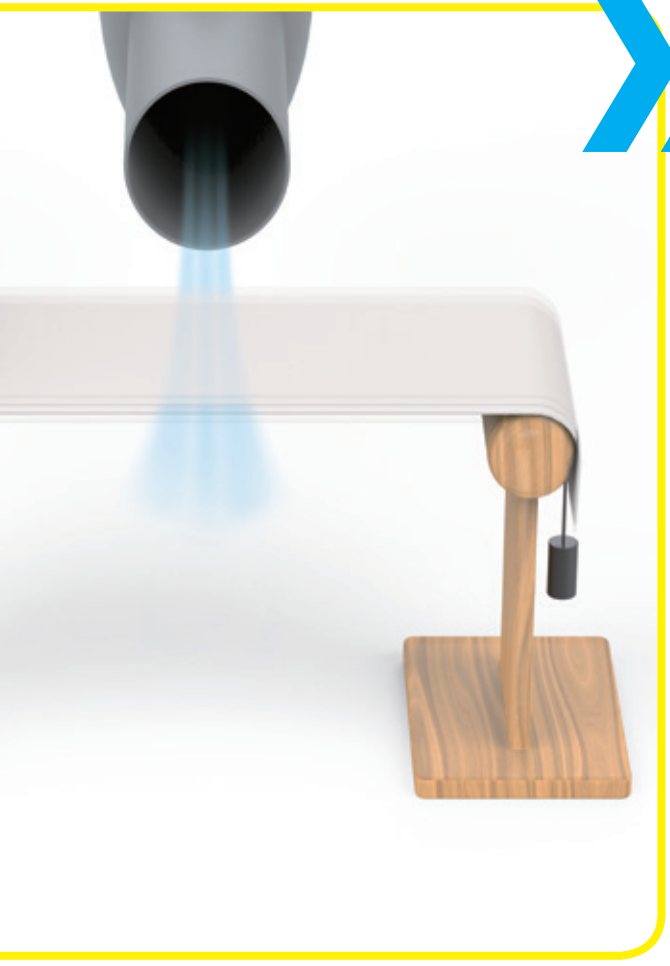

# 2015 Problem 10 : Singing Blades of Grass

## Aeroelastic Flutter with two degrees of freedom and one common frequency


### Abstract

The mechanism of how paper oscillations can produce sound is discussed, and an aeroelastic flutter model is adopted. The prediction of the fundamental frequency has also been verified extensively with the parameters – tension, paper length and mass per length- being varied in the frequency domain. The experimental setup also allows for a time domain analysis using high speed videos of the flutter. During the oscillation, two distinct freedoms of motion are observed: torsion and gallop, as predicted by the aeroelastic flutter model. The use of a sinusoidal curve fitting and torsion have shown to lead gallop, while both exhibited the same wave frequency. The results of the simulations and experiments of the paper oscillation have allowed us to ascertain the origin of the characteristic "singing" sound.



**Shen Yu Jun**
Raffles Science Institute, Raffles Institution, One Raffles Institution Lane, 575954, Singapore

**Huan Yan Qi**
California Institute of Technology, Pasadena CA 91125, United States

*yujunauthor@gmail.com*



**Keywords**

*Aeroelastic flutter, frequency, natural frequency, sound, Fast Fourier Transform*


### Introduction

When one blows across a thin blade of grass, one can hear a distinctive sound and feel the grass blade vibrating. This phenomenon may be reproduced for a paper strip, where the frequency depends on the tensional force applied to the strip. A common misconception of the cause is vortex induced vibration, which this paper will show to be insignificant. Instead, the actual mechanism responsible for the sound production is aeroelastic flutter similar to that of aeroplane wings.

The motion of paper flutter has been studied mathematically in the case of the printing press, where flutter is a dangerous problem in the paper industry to be prevented [1, 2]. In terms of biological sound generation, aeroelastic flutter has been recently proposed to be the mechanism of hummingbird feather-tip sound production. This surprising application of biological evolution allows different species of birds to generate different sound frequencies given their distinct feather shapes [3]. Furthermore, the feathers' mechanism was deduced by Clark et. al to be flutter and not vortex shedding. Aeroelastic

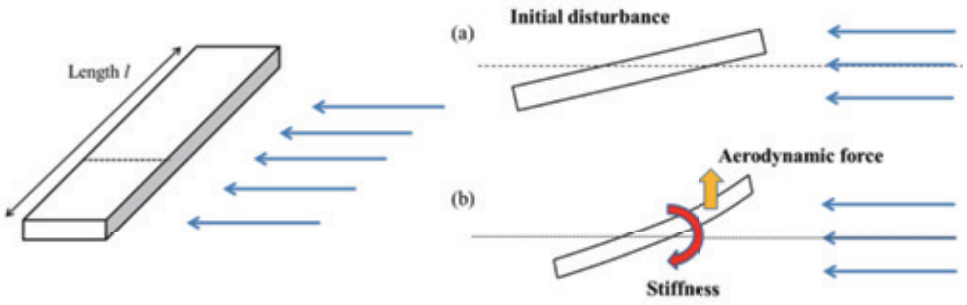


*Fig.1. Paper strip cross-section under initial excitation*

flutter of a thin, flexible material has been proposed as an environmentally-friendly and cost-effective energy generation device, especially in windy tropical countries [4]. However, the mechanism of such a wind-belt was not explained. The present solution presents a physical analogy to aerofoil flutter to explain the coupling of both gallop and torsion degrees of freedom, justifying the use of the natural frequency equation.

## Sound production mechanism

### 1. Aeroelastic flutter

The mechanism responsible for sound production is aeroelastic flutter, a form of positive feedback which leads to oscillation of the paper at its natural frequency [5]. Mechanical energy is supplied by the wind [4]. As there are visibly two degrees of freedom involved for the paper strip – up-and-down "gallop" motion and "torsion" twisting along the length – this form of flutter is similar to that of aeroplane wings. The process is illustrated in Fig. 1 with a paper strip cross-section. An initial disturbance provides an area for the wind to act upon, resulting in a pressure difference and aerodynamic force. The initial disturbance is amplified in magnitude, but is countered by torsional stiffness [5].

Once flutter is initiated, the paper strip will begin oscillating up and down as well as rotating (Fig.2) in a coupled manner. Hence, for the airfoil-type flutter, only one common frequency is expected and torsion will lead gallop motion in terms of phase difference. These two important predictions of the flutter theory can be experimentally tested.

The frequency excited will be that of the lowest energy, hence the fundamental frequency [4]. By considering the paper as a collection of strings of infinitesimal width, the natural frequency f is obtained in terms of length l (along the long edge, Fig 1), tension T and mass per length μ (Eq. 1) [5] :

$$f = \frac{1}{2l}\sqrt{\frac{T}{\mu}} \qquad (1)$$

The mass per length can be calculated by the mass per area multiplied by the width of paper strip used (e.g.

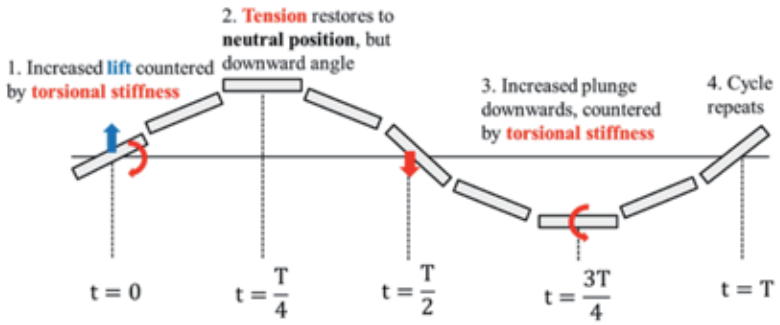


*Fig.2. Proposed mechanism for paper strip flutter. Note a common frequency is expected for both torsion and gallop modes, with torsion ahead of gallop, due to the coupled motion*

with standard office A4 paper, $=600gm^{-2}\times0.01m=6gm^{-1}$ ). Using these values, a typical flutter sound frequency is between 300 - 600 Hz.

### 2. Vortex shedding expected frequency

Vortex shedding is a phenomenon where airflow separates around a bluff body and re-forms at the rear, with a lower air pressure in the wake. This pressure difference results in an unstable, oscillatory aerodynamic pressure on the object [5, 6]. The oscillation frequency is determined by air flow velocity U, the characteristic length $\boldsymbol{l}$ of the object, and a dimensionless fluid parameter of the Strouhal number St (Eq. 2). A large Strouhal number (~1) indicates the viscosity of the fluid is dominant, while a smaller value (St <1) characterizes the buildup and swift shedding of vortices behind a bluff body. The cross section of the paper strip, along its length, is analogous to a long, thin 2D boundary across which air flows. Maximum amplitude of oscillation occurs at "lock-in", when the object resonates at the same frequency as the vortex shedding.

$$f = \frac{St \cdot U}{l} \qquad (2)$$

For the Singing Blades paper strip, the relevant Strouhal number is 0.2, the airflow velocity is near 10 m/s and the thickness of the paper is 0.5 mm. These produce an expected vortex shedding frequency of 4000 Hz. If vortex shedding is responsible for the sound produced, then the single dominant frequency would be relatively large at around 4000 Hz, while increasing the airflow velocity should increase sound frequency [2, 6]. On the other hand, the mechanism of aeroelastic flutter will generate an expected frequency between 300 – 600 Hz, much smaller than the vortex shedding frequency. Furthermore, the frequency of aeroelastic flutter does not depend on airflow velocity. These two hypotheses of frequency value and velocity dependency can be experimentally verified.

## Experiment setup

### 1. Sound recording methodology

To record the sound produced, a strip of paper was securely fastened using a clamp and tension applied to the other end via weights on a pulley (Fig. 3). Laminar airflow was incident using a nozzle connected to an air pump, and a microphone was positioned over the middle of the strip to record the sound. This setup allows the tension, paper dimensions and wind velocity to be varied individually and frequency measured. The microphone is placed closely above the centre of the paper strip in order to record large amplitude of paper oscillations while reducing the background noise or wake turbulence detected. This setup enables smooth airflow from the nozzle to the paper strip without obstruction. The sound recorded was saved to a computer and a Fast Fourier Transform (FFT) conducted digitally.

### 2 High speed tracking of flutter

In addition to frequency domain experiments, the time-domain motion of paper flutter was captured using a high speed camera. The position of various points can then be tracked to study both the gallop and torsion

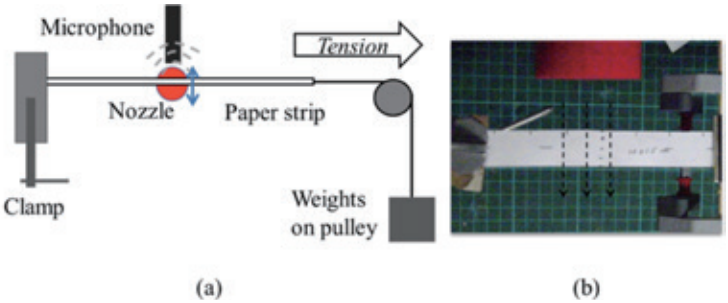


*Fig.3. Experimental setup for sound measurement (a) schematic (b) photo. Both ends of the paper strip are firmly clamped to ensure uniform tension, and the nozzle is 3D printed to deliver laminar airflow.*

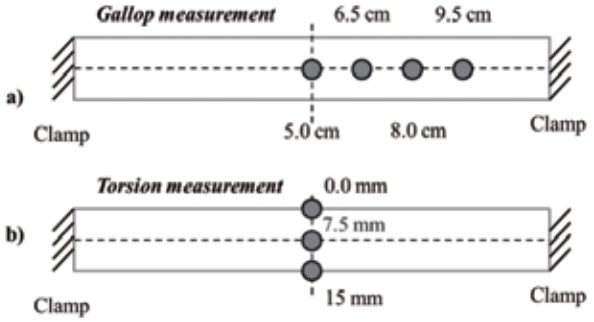


*Fig.4. Paper strip (10 cm by 1.5 cm, 70 gsm) schematic of points selected to study a) gallop and b) torsion. Note the actual displacement is the vector sum of both gallop and torsion, but the in-phase / out-of-phase motions reveal the two modes clearly.*

degrees of freedom (Fig.4) This high speed capture method allows the amplitude of oscillation to be accurately measured over time and shows the phase differences between different sections of the strip.

The motion of the side lengthwise and closer to the blower was studied for gallop motion in Fig 5a. Four points were marked, at positions 5.0 cm (middle), 6.5 cm, 8.0 cm and 9.5 cm (near the stationary end), and independently tracked. Intuitively, these points are expected to move in phase. Furthermore, torsional motion can be observed using three points along the width in the middle of the strip indicated in Fig. 5b. The positions studies were 0.00 mm point (closest to the blower), 7.50 mm point (centre) and 15.00 mm (opposite side).

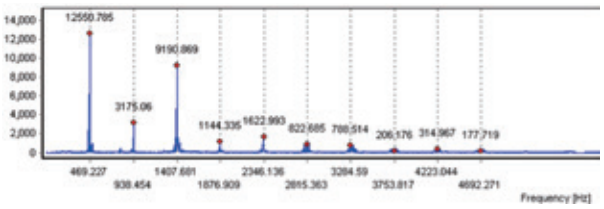


*Fig.5. Typical frequency spectrum recorded digitally after FFT, with a paper strip of 8.0 cm by 1.5 cm, 70 gsm and under 6.9 N tension. While 1st harmonic (469 Hz) is dominant, a 3rd harmonic (1407 Hz) peak exists as well (arb. units on y-axis).*

## Experiment Results

### 1. Frequency domain results from sound

From the frequency spectrum graph in Fig. 5, clear peaks can be found, such as the fundamental frequency at 469 Hz. This magnitude is expected for aeroelastic flutter, not vortex shedding.

The effect on frequency of tension, length and mass per length of the strip was studied experimentally, and compared to theoretical prediction (Fig.6). Tension was varied by placing different masses connected to the pulley, and results match prediction (Fig. 6a). The paper strip was cut to different lengths, and longer strip results in lower frequency as expected (Fig. 6b). To change the mass per length, strips of varying widths were used. A wider strip is more massive and results in lower frequency (Fig. 6c). Hence, the frequency domain results suggest the fundamental frequency is dominant, and paper oscillations are responsible for the "singing" sound.

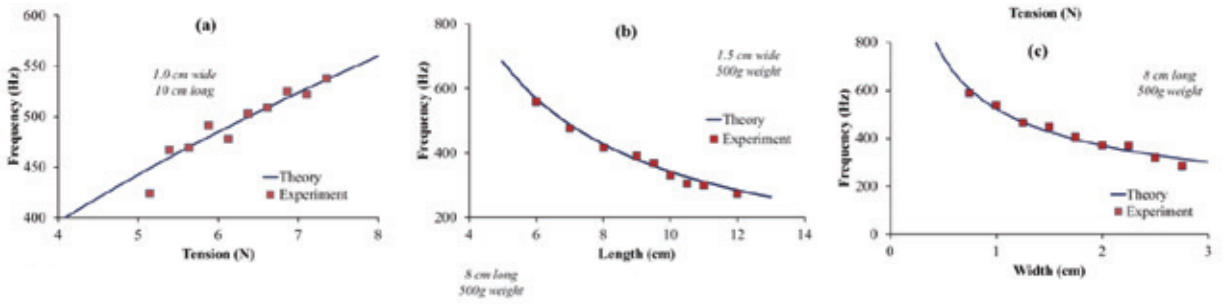


*Fig.6. Experimental results of sound frequency when Eq. 1 parameters are independently varied. (a) Tension varied, paper length of 10.0 cm and width of 1.0 cm kept constant. (b) Length varied, paper width of 1.5 cm and tension of 5.9 N kept constant. (c) Mass per length varied, paper length of 8.0 cm and tension of 5.9 N kept constant.*

In addition to the fundamental frequency, higher order harmonics are also expected. However, the position of the nozzle at the paper strip midpoint causes the centre to be an antinode, significantly reducing the 2nd harmonic. In contrast, the odd 3rd harmonic may be suitably excited. Experimentally, a peak at the 3rd harmonic peak is also observed for other paper strips of different lengths (7 – 10 cm) and tensions (500 – 700 g weights).

## 2. Time domain results from high speed tracking

The motion of the side lengthwise (using points at 5.0 cm, 6.5 cm, 8 cm and 9.5 cm) was studied for gallop motion. The oscillations of these four points were plotted across time in Fig. 7. These points along the edge oscillate in phase with each other. Furthermore, the middle 5.0 cm point has the largest magnitude of oscillation. This is indicative of an "up-and-down" gallop, although the exact amplitude is further increased by the torsional rotation.

Torsional motion was analysed using three points along the width down the middle of the strip (Fig. 8). The 0.00 mm point is closest to the blower, the 7.50 mm point in the center, and the 15.00 mm at the side away from the blower.

From the oscillation results, we observe that there is a

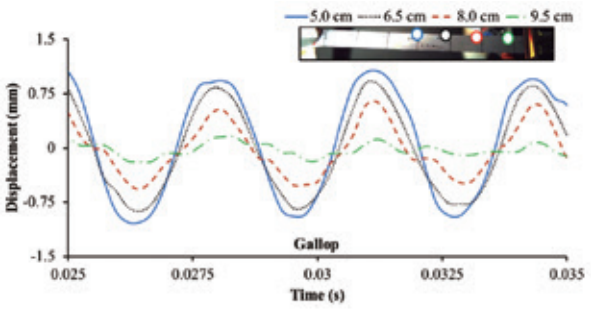


*Fig.7. Time domain result of lengthwise motion of 10.0 cm by 1.5 cm paper. The points at 5.0, 6.5, 8.0 and 9.5 all oscillate in phase, with 5.0 cm graph having the largest amplitude.*

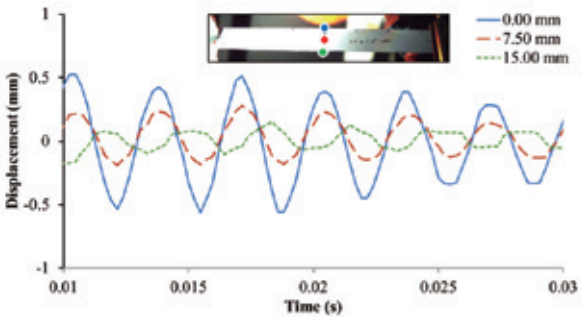


*Fig.8. Torsional motion of 10.0 cm by 1.5 cm paper. The points at 0.00 mm, 7.5 mm and 15.00 mm oscillate out of phase as predicted, due to the rotation of paper in this second degree of freedom.*

clear phase lag between the two free edges of the paper, showing a torsional "twisting" motion (0.00 mm line and 15.00 mm line). In addition, the side nearer the blower oscillates with larger amplitude than the other end. This is due to the rapid attenuation of airflow velocity across the paper obstacle; with a larger wind velocity at the 0.00 mm, it oscillates more.

From the high speed video recordings, the oscillations in gallop and torsion modes can each be fitted to a sinusoidal curve. Assuming a linear superposition of these two independent degrees of freedom, the resultant displacement of any point on the paper is the sum of these two modes at one particular time. Furthermore, the relative phase difference between the gallop and torsion modes can be fitted, to compare against the airfoil flutter model (Eq. 3).

$$z = A_g \sin(\omega_g t - \phi_g) \sin\left(\frac{\pi x}{L}\right) + A_t \left(\frac{y - y_0}{y}\right) \sin(\omega_t t - \phi_t) \sin\left(\frac{\pi x}{L}\right) \quad (3)$$

Here, the amplitudes of gallop and torsion are $A_g$ and $A_t$, and the wave frequencies are $\omega_g$ and $\omega_t$ respectively. The phase terms are $\phi_g$ and $\phi_t$, which show whether torsion or gallop is ahead in phase of the other. Finally, the half-wave envelope is considered via the $\sin\left(\frac{\pi x}{L}\right)$ term, as the strip is clamped at two ends. This form supposes linear superposition of the gallop and torsion modes. The fits for the paper middle (7.5 mm) and edge

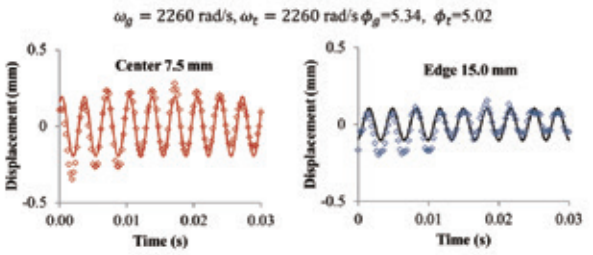


*Fig.9. Experimental fitting of paper motion to obtain the angular frequencies and phase constants.*

(15.0 mm) are shown in Fig. 9, together with fitted constants.

This fit considers both torsion and gallop, and these two are shown to have the same angular frequency of 2260 rad/s. Interestingly, both modes oscillate at the same rate, which is expected in the airfoil flutter mechanism of Section 2.1. This particular form of aeroelastic oscillation requires both gallop and torsion modes to exist and interact, leading to the same angular frequency. In terms of sound, this corresponds to 360 Hz -- as expected for an audible paper "singing" tone. Furthermore, the fit parameter $\phi_g$ (5.34 rad) is larger than $\phi_t$ (5.02 rad), showing that torsion leads gallop as predicted by the flutter theory.

## 3. Effect of airflow velocity

For a self-excited oscillation, the magnitude of disturbing force only affects the magnitude of oscillations' displacement and not the frequency. Thus, blowing the paper strip at higher velocities should increase amplitude of the sound detected but not the FFT results. Experimental photographs of the flutter envelope at a higher airflow velocity verify this hypothesis (Fig 4.)

The shape of the paper at increasing airflow velocities was tracked, showing that the amplitude of oscillation clearly increases with faster airflow velocities (Fig. 11a). Furthermore, the frequency spectrum of the same experiments show little change

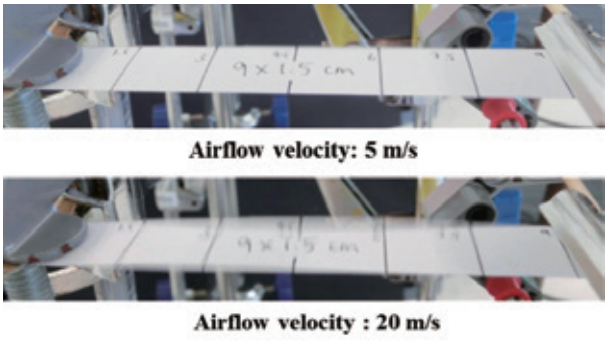


*Fig.10. Experiment photographs of larger flutter envelope at higher airflow velocities*

in sound quality produced (Fig. 11b). All three FFT spectrums show a dominant fundamental frequency and a smaller 3rd harmonic. The slight deviation of the medium velocity result may be caused by higher-order hysteresis effects during experiment of repeated loadings. This behaviour does not support vortex shedding, where the frequency is dependent on flow velocity [6]. Since the velocity of blowing only affects magnitude of oscillation, the mechanism is the self-excitation of paper flutter.

## Discussion

Comparing multiple results for one set of experiments, it can be shown paper flutter is responsible for the sound production. For a paper of length 10.0 cm, width 1.5 cm and mass per length

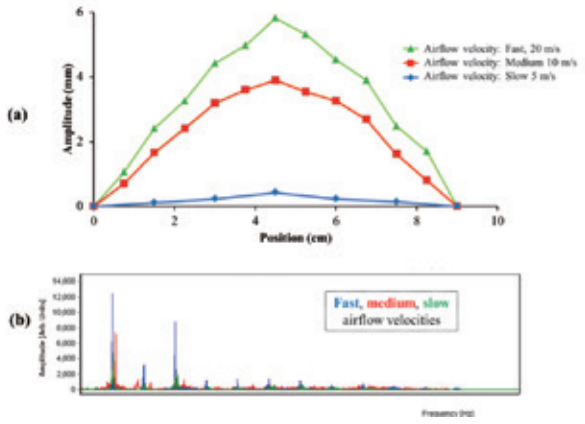


*Fig.11. Empirical results of increasing airflow velocities for 9.0 cm by 1.5 cm, 500gsm paper at 5.9 N. Blue, red and green plots correspond to the fast (~20 m/s), medium (~10 m/s) and slow (~5 m/s) airflows. (a) Higher airflow velocities correspond to larger amplitude of oscillation but has (b) negligible effect on frequency spectrum.*

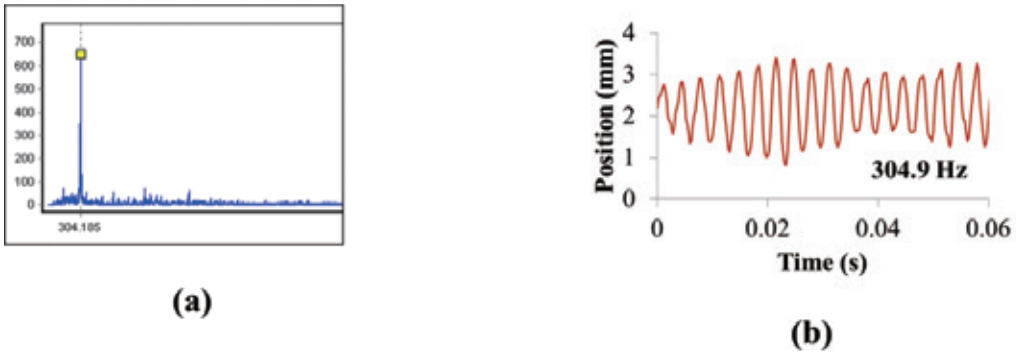


*Fig.12. Match between experimental results of paper motion. (a) FFT of sound recorded (frequency domain) shows dominant frequency of 304.2 Hz. (b) From high speed video (time domain), the paper flutters at 304.9 Hz. The theoretical value is 305 Hz.*

700 gsm (typical office A4 paper), the fundamental frequency expected for flutter using Eq. 1 is 305 Hz. The experiment was conducted with the sound recorded by a microphone and motion captured by a high speed camera. In the frequency domain (sound, Fig. 12a), the dominant frequency was found to be 304.2 Hz; in the time domain (motion, Fig. 12b), the dominant frequency in the oscillation was found to be 304.9 Hz. These values agree well the predicted theoretical frequency above.

Indeed, vortex shedding would result in a single degree of freedom "gallop" motion only – for example, the motion of power cables which may also produce a "singing" sound. In some experiments, the paper was observed to flutter to the breaking point, showing the stresses exerted were too large for the material strength [1]. This is qualitatively similar to the breaking of the Tacoma Narrows Bridge, caused by excessive torsional oscillation [5].

## Conclusion

The mechanism of paper oscillation producing sound was discussed and an aeroelastic flutter model was adopted. The prediction of fundamental frequency excited was verified extensively with all parameters– tension, paper length and mass per length– varied in the frequency domain. The experimental setup also allows for a time domain analysis using high speed videos of the flutter. During the oscillation, two distinct freedoms of motion were observed: torsion and gallop, as predicted by the aeroelastic flutter model. Sinusoidal curve fitting was used and torsion was shown to lead gallop, while both exhibited the same wave frequency. Through extensive experimental investigation of this problem, paper oscillation was proven to be responsible for the characteristic "singing" sound detected.

## Acknowledgements

The research work was carried out in preparation for the 28th International Young Physicists' Tournament at Raffles Institution, Singapore. The authors gratefully acknowledge the guidance of the teachers Mr Sze Guan Kheng, Mrs Lim Siew Eng and Mr Calvin Tan from Raffles Institution, and the invaluable assistance of Dr Tan Guoxian from Raffles Science Institute for helping to prepare this manuscript in submission to the IYPT magazine. The kind assistance of Miss Siti, Miss Farah and Miss Doris from Raffles Science Institute in preparing the experimental setups is also deeply appreciated by the authors. The authors would also like to acknowledge the fruitful discussions with the IYPT Singapore team members and coaches during the competition preparation.

## *References*

1. Y. Watanabe, K. Isogai, S. Suzuki, and M. Sugihara, A Theoretical Study of Paper Flutter. Journal of Fluids and Structures, 2002(16(4)): p. 543–560.

2. Y. Watanabe, S. Suzuki, M. Sugihara, and Y. Sueoka, An Experimental Study of Paper Flutter. Journal of Fluids and Structures, 2002. 16(4), 529-542.

3. C. J. Clark, D. O. Elias, M. B. Girad, and R. O. Prum, Structural resonance and mode of flutter of hummingbird tail feathers. Journal of Experimental Biology, 2013. 216(18), 3404-3413.

4. E. Arroyo, S. Foong, and K. L. Wood, Modeling and experimental characterization of a fluttering windbelt for energy harvesting. Journal of Physics: Conference Series, 2014. (Vol. 557, No. 1, p. 012089). IOP Publishing.

5. J. P. D. Hartog, Mechanical Vibrations. 1956: McGraw-Hill Book Company.

6. Y. Nakamura, Y. Ohya, S. Ozono, and R. Nakayama, Experimental and numerical analysis of vortex shedding from elongated rectangular cylinders at low Reynolds numbers 200-1000. Journal of Wind Engineering and Industrial Aerodynamics, 1996. 65(1), 301-308.